Rapid-repeat time lapse seismic VSP imaging of CO_2 injection

Xiaohui Cai[1], Kristopher A. Innanen[1], Qi Hu[1], Scott D. Keating[1], Matthew V. Eaid[1], and Donald C Lawton[2]

[1] *Dept. of Geoscience, CREWES Project, University of Calgary*

[2] *Containment and Monitoring Institute, Carbon Management Canada*

Summary

Carbon capture and storage (CCS) is widely recognized as having potential in meeting climate change goals. Monitoring injected CO_2 is a major concern for CCS, here we use elastic full waveform inversion (FWI) to detect injected CO_2 transient change from rapid-repeat time-lapse VSP data. The elastic FWI workflow mainly consists of three steps: a P-wave velocity single-parameter frequency-domain inversion, effective source estimation and time-lapse strategy. The field data application implies that our rapid-repeat time-lapse inversion scheme is able to detect the CO_2 transient change.

Workflow

A P-wave velocity single-parameter frequency-domain inversion

We perform the 2D elastic frequency-domain FWI algorithm combined geophone and DAS data (Eaid et al., 2020). The P-wave and (V_P), S-wave velocity (V_S), and density (ρ) show strong correlation in our data, therefore we use the single parameter V_P to implement the 2D elastic frequency-domain FWI, which could apply the prior information in the inversion and help prevent cross-talk by only allowing updates in one parameter. The V_S and ρ could be obtained by the relationship with the V_P.

Effective source estimation

In our current study, to avoid the near surface from the inversion problem, we use the effective sources approach (Keating et al., 2021) for VSP FWI.

Time-Lapse Strategy

There are different inversion strategies that can be used to estimate the time-lapse changes in the medium, such as Parallel strategy, Sequential strategy, Double-difference strategy (Asnaashari et al., 2015). For the field data set here, rapid-repeat time-lapse data is characterized by multiple repetitions in a short period of time. Therefore, the differences between the baseline and monitor data are mainly caused by the changes in the medium, while the changes due to the differences in source and receiver could be negligible. Here, we adopt the Parallel strategy， where both the baseline and the monitor inversions use the same inversion parameters and the same effective source energy.

Field Data Inversion

Data

In January 2022, the Containment and Monitoring Institute Newell County Facility, carried out a rapid-repeat time-lapse VSP seismic experiment (named Tiny bubbles) near Brooks, Alberta. The

CO_2 was injected into a shallow formation at a depth of 300 meters (Isaac and Lawton, 2016), and repeated a seismic shot whose ray-paths crossed the expected fluid, seeking evidence of transient changes. Geometry of the experiment is summarized in Figure 1. The CO_2 entered the Basal Belly River Sandstone (BBRS) formation, forming pressure and fluid plumes between depths of 290-305 m. The 24 3C geophones were located from 190 m to 305 m with interval of 5 m, while the DAS fiber were located from 0 m to 337 m. The source was 215 m away from the observation well, and injection well located between the source and observation well. In addition, the estimated pressure plume located at injection well at 267 m, where the pressure changes are shown in Figure 2. Based on the rapid-repeat seismic shots, about 20 shots with good repeatability in a short period of time are grouped into a cluster, and there are 64 clusters in total.

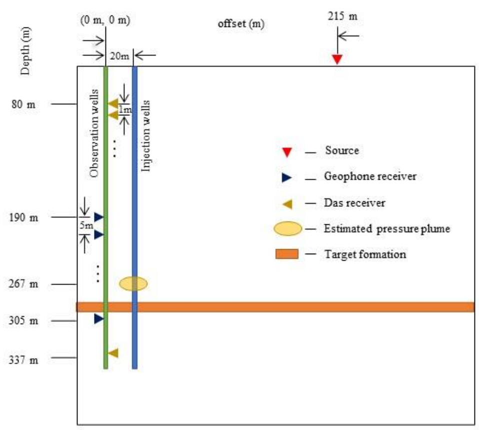

Figure 1: Geometry of Tiny bubbles seismic source, injection, and observation wells.

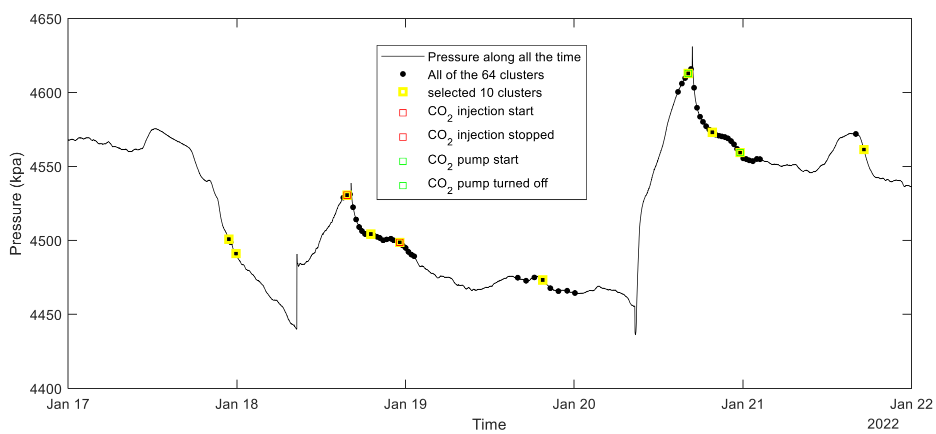

Figure 2: Pressure change at 267 m (black curve) along the time from Jan 17 to Jan 22, 2022. Black circles are the times at which all 64 monitoring shot clusters occurred. Red squares and green squares indicate the first and second time CO_2 injection, respectively.

Preprocessing

Preprocessing is performed before the inversion, where the preprocessing workflow has shown in Figure 3.

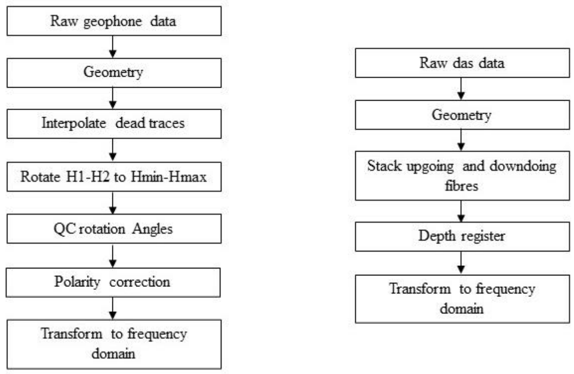

Figure 3: Preprocessing workflow of the geophone data (left) and DAS data (right).

Results

To quantitative analyze the difference between monitor clusters and baseline cluster, we calculate the normalization of their differences between the monitor and baseline data for vertical geophone component, horizontal geophone component and DAS data (Figure 4). It can be seen from the normalization figures, the anomaly values appear around 285 m and 300 m in vertical component, and almost appear 285-290 m in horizontal component. The DAS normalized value does not show significant difference.

The initial and inverted models of V_P, V_S, and ρ for baseline is shown in Figure 5. The model size is 240 m in the x-direction and 350 m in the z-direction, and the space interval is 2.5 m. In this report, we focus on frequencies between 10 Hz and 25 Hz. The inversion approach could be divided into two steps: first is the source-only inversion based on baseline data and second is the model-only inversion for all the 64 clusters data. Figure 6 show the time-lapse V_P models, and amplitude of time-lapse anomaly is different from the noise and the time-lapse anomaly is located around 287.5 m, which have a good consistency with the field data normalization in Figure 4. Based on the phenomenon, we extract the inversion time-lapse V_P model value located (25 m, 287.5 m) for all 64 clusters. Figure 7 shows pressure data and inverted time-lapse V_P models for all the 64 clusters. It can be seen that the inverted V_P keep decreasing with the first CO_2 injection, and then it reaches a relatively stable stage, there is a certain ups and downs during the second CO_2 injection, and the overall trend is downward, finally it tries to return to initial state. The time-lapse V_P anomaly varies between 0 and 150 m/s.

Conclusions

We provide the rapid-repeat time-lapse velocity model inversion based on Tiny bubbles data. We use log-derived P-wave velocity single-parameter to help model convergence and explain the data as a full multi-parameter inversion. In addition, the effective source approach is introduced to avoid many complications in near-surface land seismic data. The results of 2D elastic FWI on field and synthetic offset VSP data show that this technology can provide high-resolution models of physical properties of the subsurface, detecting and quantifying the anomaly. Our results show that FWI of VSP data is a suitable tool for the monitoring of CO2 geosequestration and transportation.

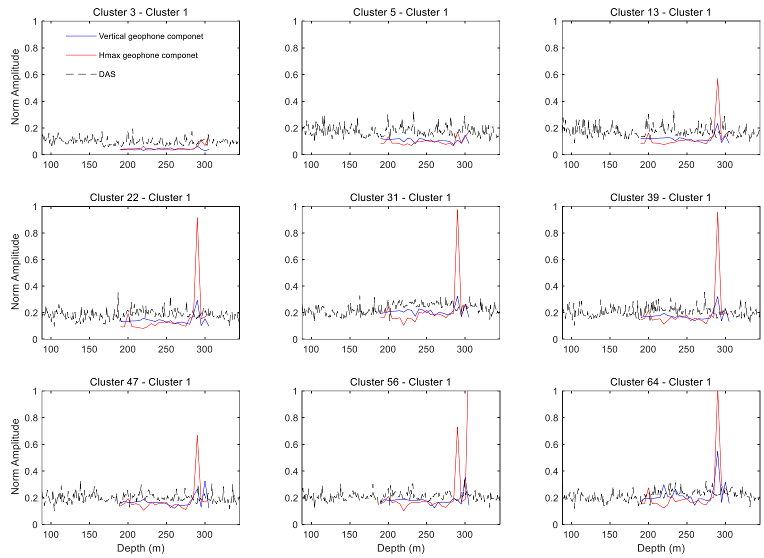

Figure 4: The normalization of difference between monitor data and baseline data.

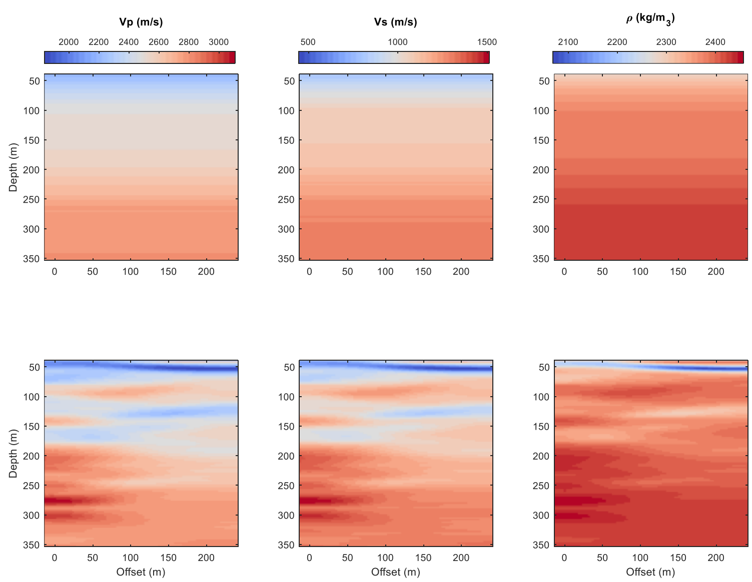

FIG. 5. Initial and inverted models of V_P, V_S, and ρ for cluster 1 (baseline data).

Acknowledgements

This work was funded by CREWES industrial sponsors and NSERC (Natural Science and Engineering Research Council of Canada) through the grant CRDPJ 543578-19. The data were acquired through a collaboration with the Containment and Monitoring Institute, Carbon Management Canada. The first author was partially supported by a scholarship from the SEG Foundation.

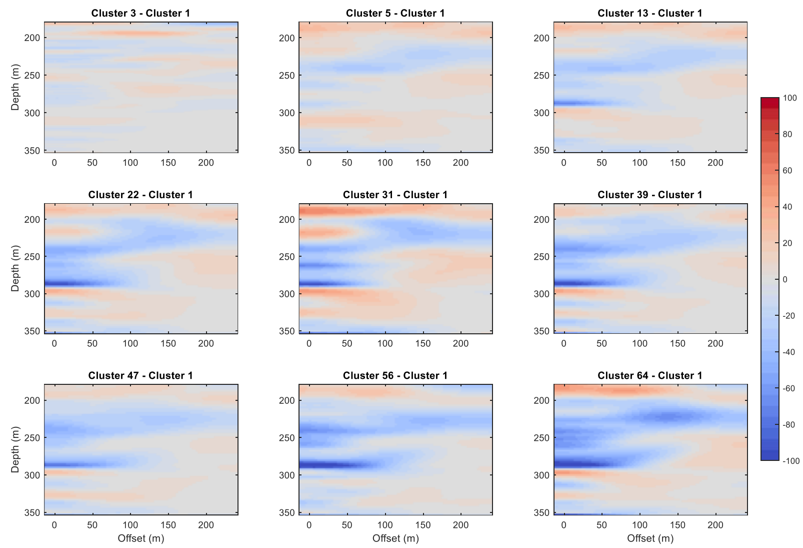

FIG. 6. The inverted V_P models difference between the 9 monitor data and baseline.

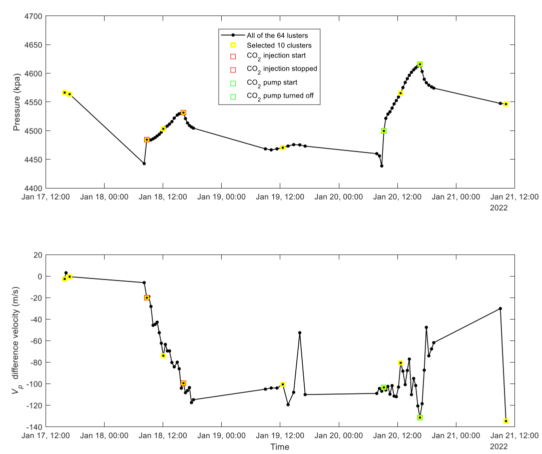

FIG. 7. Top rows: Pressure data at 267 m (black curve) for the 64 clusters. Bottom rows: The inverted V_P models difference between the 64 clusters and baseline data at 287.5 m. Yellow square are the 10 selected clusters. Red squares and green squares indicate the first and second CO_2 injection, respectively.

References

Asnaashari, A., Brossier, R., Garambois, S., Audebert, F., Thore, P., and Virieux, J., 2015, Time-lapse seismic imaging using regularized full-waveform inversion with a prior model: which strategy?: Geophysical prospecting, 63, No. 1, 78–98.

Eaid, Matthew V., Scott D. Keating, and Kristopher A. Innanen., 2020, Multiparameter seismic elastic full-waveform inversion with combined geophone and shaped fiber-optic cable data: Geophysics 85, No. 6, R537-R552.

Isaac, J. H., and Lawton, D. C., 2016, Brooks revisited: CREWES Research Reports.

Keating, S., Eaid, M., and Innanen, K., 2021, Effective sources: removing the near surface from the vsp fwi problem: CREWES Report.